Reaction of 1-(Dimethylsilyl)-2-silylbenzene with Platinum(0) Phosphine Complexes

Shigeru Shimada,*[,†] Maddali L. N. Rao,[†,§] Yong-Hua Li,[†] and Masato Tanaka*[,†,‡]

National Institute of Advanced Industrial Science and Technology (AIST), Tsukuba Central 5, 1-1-1 Higashi, Tsukuba, Ibaraki 305-8565, Japan, and Chemical Resources Laboratory, Tokyo Institute of Technology, Nagatsuta, Midori-ku, Yokohama 226-8503, Japan

Received June 15, 2005

Reaction of 1,2-$C_6H_4(SiMe_2H)(SiH_3)$ (**8**) with $Pt(dmpe)(PEt_3)_2$ (dmpe = $Me_2PCH_2CH_2PMe_2$) or $Pt(dmpe)_2$ in 1:1 ratio at room temperature gave $\{1,2\text{-}C_6H_4(SiMe_2)(SiH_2)\}Pt^{II}(dmpe)$ (**11a**) as a major product in solution. Complex **11a** can easily dimerize to form $[(dmpe)Pt^{IV}(H)\{1,2\text{-}C_6H_4(SiMe_2)(\mu\text{-}SiH)\}]_2$ (**12a**), and **11a** and **12a** are in equilibrium in solution. Although monomer **11a** is a major species in solution, only dimer **12a** crystallized out from toluene, THF, or DMF solution. Addition of excess dmpe to a toluene solution of **11a/12a** trapped the Pt^{II} species as a pentacoordinated dimer $[\{1,2\text{-}C_6H_4(SiMe_2)(SiH_2)\}Pt^{II}(dmpe)]_2(\mu\text{-}dmpe)$ (**13**). A similar reaction took place between **8** and $Pt(depe)(PEt_3)_2$ (depe = $Et_2PCH_2CH_2PEt_2$) or $Pt(depe)_2$ to give $\{1,2\text{-}C_6H_4(SiMe_2)(SiH_2)\}Pt^{II}(depe)$ (**11b**) and $[(depe)Pt^{IV}(H)\{1,2\text{-}C_6H_4(SiMe_2)(\mu\text{-}SiH)\}]_2$ (**12b**), and **11b** and **12b** are in equilibrium in solution. Two equivalents of **8** reacted with $Pt(dmpe)(PEt_3)_2$ in toluene at room temperature to afford two isomeric $\{1,2\text{-}C_6H_4(SiMe_2H)(SiH_2)\}\{1,2\text{-}C_6H_4(SiMe_2)(SiH_2)\}(H)Pt^{IV}(dmpe)$ complexes **16** and **17** in 5:3 ratio among eight possible isomers. Heating the mixture of **16** and **17** at 100 °C in toluene resulted in slow intramolecular dehydrogenative cyclization to afford a mixture of isomeric $\{1,2\text{-}C_6H_4(SiMe_2)(SiH_2)\}_2Pt^{IV}(dmpe)$ **18** and **19**. The structures of complexes **12a**, **12b**, **13**, **17**, **18**, and **19** were unambiguously determined by single-crystal X-ray analysis.

Introduction

The reaction chemistry of transition-metal complexes with primary and secondary hydrosilanes ($RSiH_3$ and R_2SiH_2) has been rapidly growing recently. It is often different from that with tertiary hydrosilanes (R_3SiH) because primary and secondary hydrosilanes have more than one reactive Si−H bond and/or are sterically less hindered than tertiary hydrosilanes.[1] The reaction of Pt(0) complexes with tertiary hydrosilanes usually produces (silyl)(hydrido)platinum(II) and/or bis(silyl)-platinum(II) complexes,[1] while that with primary and secondary hydrosilanes affords various types of platinum(II) and platinum(IV) complexes with mononuclear,[1] dinuclear,[1−7] or trinuclear[8,9] frameworks. We have been studying the reactivity of chelating hydrosilanes such as 1,2-$C_6H_4(SiH_3)_2$[10,11] and $[2\text{-}(SiH_3)C_6H_4]_2SiH_2$[12] with group 10 metal complexes and disclosed the formation of a number of unique complexes with silicon−metal bonds.

The reaction of 1,2-bis(dimethylsilyl)benzene (**1**) with $Pt(CH_2{=}CH_2)(PPh_3)_2$ affords bis(silyl)platinum(II) complex **2** exclusively, and no further reaction of **2** with a

* Corresponding authors. Fax: +81-29-861-4511. Tel: +81-29-861-6257. E-mail: s-shimada@aist.go.jp (S.S.); m.tanaka@res.titech.ac.jp (M.T.).

† National Institute of Advanced Industrial Science and Technology (AIST).

‡ Tokyo Institute of Technology.

§ Present address: Department of Chemistry, Indian Institute of Technology, Kanpur, Kanpur 208016, India.

(1) For recent reviews: (a) Eisen, M. S. In *The Chemistry of Organic Silicon Compounds*; Rappoport, Z., Apeloig, Y., Eds.; John Wiley & Sons: New York, 1998; Vol. 2, Part 3, Chapter 35. (b) Ogino, H.; Tobita, H. *Adv. Organomet. Chem.* **1998**, *42*, 223−290. (c) Corey, J. Y.; Braddock-Wilking, J. *Chem. Rev.* **1999**, *99*, 175−292.

(2) Auburn, M.; Ciriano, M.; Howard, J. A. K.; Murray, M.; Pugh, N. J.; Spencer, J. L.; Stone, F. G. A.; Woodward, P. *J. Chem. Soc., Dalton Trans.* **1980**, 659−666.

(3) (a) Zarate, E. A.; Tessier-Youngs, C. A.; Youngs, W. J. *J. Am. Chem. Soc.* **1988**, *110*, 4068−4070. (b) Zarate, E. A.; Tessier-Youngs, C. A.; Youngs, W. J. *J. Chem. Soc., Chem. Commun.* **1989**, 577−578. (c) Sanow, L. M.; Chai, M. H.; McConnville, D. B.; Galat, K. J.; Simons, R. S.; Rinaldi, P. L.; Youngs, W. J.; Tessier, C. A. *Organometallics* **2000**, *19*, 192−205.

(4) Heyn, R. H.; Tilley, T. D. *J. Am. Chem. Soc.* **1992**, *114*, 1917−1919.

(5) Michalczyk, M. J.; Recatto, C. A.; Calabrese, J. C.; Fink, M. J. *J. Am. Chem. Soc.* **1992**, *114*, 7955−7957.

(6) (a) Levchinsky, Y.; Rath, N. P.; Braddock-Wilking, J. *Organometallics* **1999**, *18*, 2583−2586. (b) Braddock-Wilking, J.; Levchinsky, Y.; Rath, N. P. *Organometallics* **2000**, *19*, 5500−5510. (c) Braddock-Wilking, J.; Levchinsky, Y.; Rath, N. P. *Organometallics* **2001**, *20*, 474−480. (d) Braddock-Wilking, J.; Levchinsky, Y.; Rath, N. P. *Inorg. Chim. Acta* **2002**, *330*, 82−88.

(7) (a) Tanabe, M.; Osakada, K. *Inorg. Chim. Acta* **2003**, *350*, 201−208. (b) Tanabe, M.; Yamada, T.; Osakada, K. *Organometallics* **2003**, *22*, 2190−2192.

(8) Osakada, K.; Tanabe, M.; Tanase, T. *Angew. Chem., Int. Ed.* **2000**, *39*, 4053−4055.

(9) (a) Braddock-Wilking, J.; Corey, J. Y.; Dill, K.; Rath, N. P. *Organometallics* **2002**, *21*, 5467−5469. (b) Braddock-Wilking, J.; Corey, J. Y.; Trankler, K. A.; Dill, K. M.; French, L. M.; Rath, N. P. *Organometallics* **2004**, *23*, 4576−4584.

(10) (a) Shimada, S.; Tanaka, M.; Honda, K. *J. Am. Chem. Soc.* **1995**, *117*, 8289−8290. (b) Shimada, S.; Tanaka, M.; Shiro, M. *Angew. Chem., Int. Ed. Engl.* **1996**, *35*, 1856−1858. (c) Shimada, S.; Rao, M. L. N.; Tanaka, M. *Organometallics* **1999**, *18*, 291−293. (d) Shimada, S.; Rao, M. L. N.; Hayashi, T.; Tanaka, M. *Angew. Chem., Int. Ed.* **2001**, *40*, 213-216. (e) Chen, W. Z.; Shimada, S.; Tanaka, M. *Science* **2002**, *295*, 308−310.

(11) (a) Schröck, R.; Sladek, A.; Schmidbaur, H. *Z. Naturforsch. B* **1994**, *49*, 1036−1040. (b) Minge, O.; Nogai, S.; Schmidbaur, H. *Z. Naturforsch. B* **2004**, *59*, 153−160.

(12) (a) Chen, W. Z.; Shimada, S.; Hayashi, T.; Tanaka, M. *Chem. Lett.* **2001**, 1096−1097. (b) Chen, W. Z.; Shimada, S.; Tanaka, M.; Kobayashi, Y.; Saigo, K. *J. Am. Chem. Soc.* **2004**, *126*, 8072−8073.

10.1021/om050498j CCC: $30.25 © 2005 American Chemical Society
Publication on Web 10/22/2005

Scheme 1

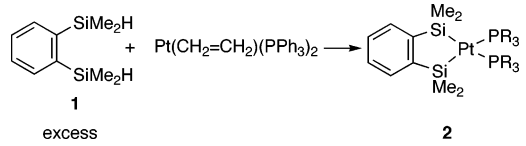

Scheme 2

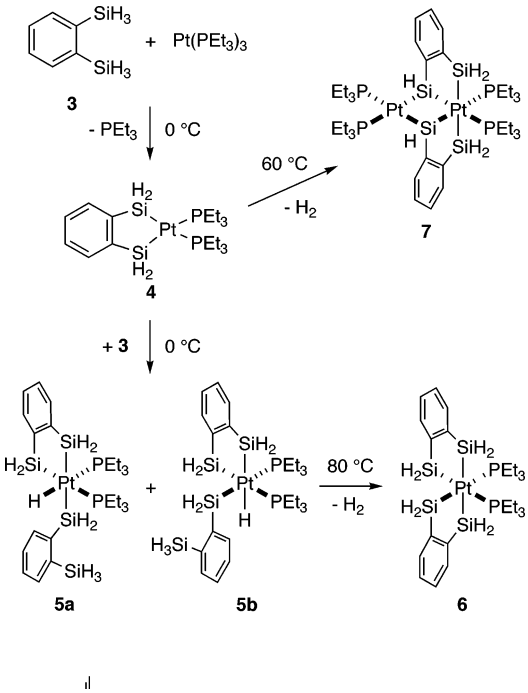

second molecule of **1** takes place (Scheme 1).[13] We have previously reported that when all the methyl groups on Si atoms in **1** are replaced with hydrogen atoms, the reaction of the hydrosilane with platinum(0) complexes became much more complicated (Scheme 2).[10a] The reaction of hydrosilane **3** with platinum(0) phosphine complex in 1:1 ratio at 0 °C gives bis(silyl)platinum(II) complex **4**. However, complex **4** can easily react with another molecule of **3** to form tris(silyl)(hydrido)platinum(IV) complexes as a mixture of isomers **5a** and **5b**, which are upon heating further transformed to tetrakis(silyl)platinum(IV) complex **6**. In the absence of another molecule of **3**, complex **4** dimerizes to form mixed-valent $Pt^{II}Pt^{IV}$ complex **7**. The decrease in steric bulkiness and the existence of extra Si−H bonds make the reaction of **3** with platinum(0) complex more complicated. In this paper, we describe the reaction of 1-(dimethylsilyl)-2-silylbenzene (**8**), which is a hybrid of **1** and **3**, with platinum(0) phosphine complexes, which clearly reflects the steric effects of silyl groups.

Results and Discussion

The reaction of **8** with platinum complex **9a** or **10a** in a 1:1 ratio in toluene proceeded at room temperature to give a colorless solid in high yield, whose NMR spectra in THF-d_8 showed the formation of bis(silyl)-platinum(II) complex **11a** as a major product together with a small quantity of **12a** (Scheme 3, **11a/12a** = ca. 95/5 by ^{1}H and ^{31}P{^{1}H} NMR integrations in THF-d_8).

Scheme 3

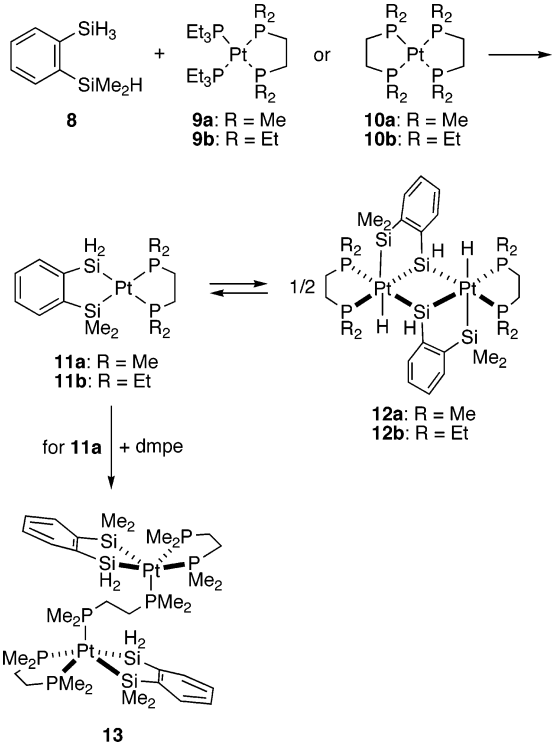

Dinuclear complex **12a** is a dimer of **11a**, and **11a** and **12a** have proved to be in equilibrium in solution (vide infra). The ^{31}P{^{1}H} NMR spectrum of the product in THF-d_8 (Figure 1) showed a pair of doublets at 39.5 ppm ($^1J_{Pt-P}$ = 1623 Hz) and 40.0 ppm ($^1J_{Pt-P}$ = 1337 Hz) for the major species, $^1J_{Pt-P}$ values of which are within the typical range of those observed in *cis*-bis(silyl)bis(phosphine)platinum(II) complexes,[4,6b,10a,14] supporting the formation of **11a**. In the ^{1}H NMR spectrum, the major species displayed a signal for SiH_2 as a triplet ($^3J_{P-H}$ = 7 Hz) with Pt and Si satellites ($^2J_{Pt-H}$ = 22 Hz, $^1J_{Si-H}$ = 159 Hz) as observed in *cis*-$(Ph_3P)_2Pt[SiH_2(p\text{-Tol})]_2$.[6b]

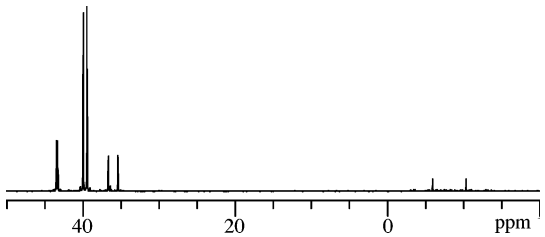

Figure 1. ^{31}P{^{1}H} NMR spectrum of **11a/12a** in THF-d_8 solution.

Despite the low concentration of the minor product, recrystallization of the product mixture from toluene, THF, or DMF afforded only crystals of **12a**. Single-crystal X-ray analysis unambiguously confirmed the structure of **12a** (vide infra). ^{1}H and ^{31}P NMR signals of the minor species in solution are consistent with the structure of **12a**.The ^{1}H NMR spectrum showed a weak

(13) Eaborn, C.; Metham, T. N.; Pidcock, A. *J. Organomet. Chem.* **1973**, *63*, 107−117.

(14) (a) Eaborn, C.; Metham, T. N.; Pidcock, A. *J. Chem. Soc., Dalton Trans.* **1975**, 2212−2214. (b) Eaborn, C.; Metham, T. N.; Pidcock, A. *J. Organomet. Chem.* **1977**, *131*, 377−385. (c) Holmes-Smith, R. D.; Stobart, S. R.; Cameron, T. S.; Jochem, K. *J. Chem. Soc., Chem. Commun.* **1981**, 937−939. (d) Kobayashi, T.; Hayashi, T.; Yamashita, H.; Tanaka, M. *Chem. Lett.* **1988**, 1411−1414.

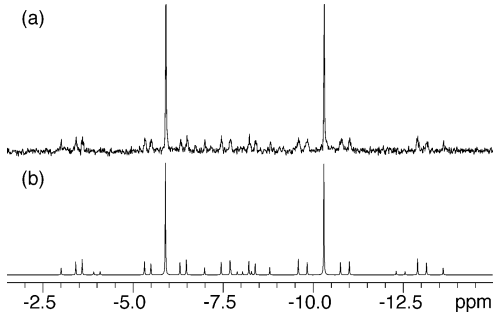

Figure 2. $^{31}P\{^1H\}$ NMR spectra of **12a**. (a) −15 to −1.5 ppm region of Figure 1. (b) Simulated spectrum.

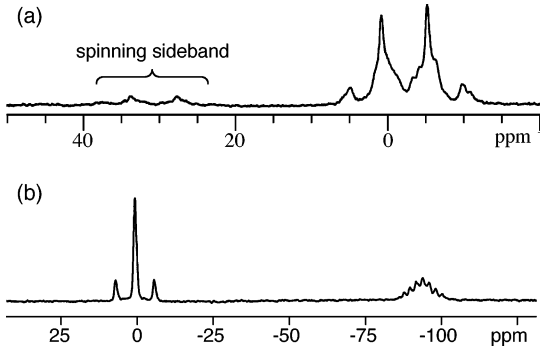

Figure 3. Solid-state NMR spectra of **12a**. (a) $^{31}P\{^1H\}$ CP/MAS spectrum. (b) $^{29}Si\{^1H\}$ CP/MAS spectrum.

signal at −8.6 ppm assignable to Pt−*H*. The $^{31}P\{^1H\}$ NMR spectrum showed a AA′BB′XX′ pattern for the minor species (Figure 2a), where X and X′ are platinum atoms. Figure 2b is a simulated $^{31}P\{^1H\}$ NMR spectrum of **12a**.[15] Most of the signals in the simulated spectrum are observed in the measured spectrum. Since the single-crystal X-ray analysis cannot rule out the possibility that the crystals are a mixture of complexes **11a** and **12a**, the homogeneity of the crystals was confirmed by solid-state NMR spectroscopy. Figure 3 shows CP/MAS $^{31}P\{^1H\}$ and $^{29}Si\{^1H\}$ NMR spectra and is clearly showing that the crystals are not a mixture of **11a** and **12a** but are pure **12a**. The CP/MAS $^{31}P\{^1H\}$ NMR spectrum (Figure 3a) showed two signals at the position near those for the minor product observed in the $^{31}P\{^1H\}$ NMR spectrum of a mixture of **11a** and **12a** in THF-d_8. The CP/MAS $^{29}Si\{^1H\}$ NMR spectrum (Figure 3b) showed two signals at −94.0 and 0.7 ppm. The former signal is assignable to the silicon atoms of Si_2Pt_2 four-membered cycles; the high-field value is typical for the Si_2Pt_2 four-membered cycles **14** with short diagonal Si···Si distances.[3c,6,10a] Each Pt center in complex **12a** forms $(Si)_3(H)Pt^{IV}$; a similar situation is found in Tilley's complex **15**, where both hydrido ligands occupy the same side of the Si_2Pt_2 ring.[4]

Although monomer **11a** could not be obtained as a crystal, **11a** can be trapped by an extra dmpe ligand (Scheme 3); addition of excess dmpe to a mixture of **11a/12a** in toluene afforded a small amount of crystals, whose structure was confirmed by X-ray analysis to be a μ-dmpe-bridged dimer **13** (vide infra).

A similar reaction takes place between **8** and depe complex **9b** or **10b**, giving bis(silyl) complex **11b** as a major product in solution (^{31}P NMR in THF-d_8: δ 64.5 ($^1J_{Pt-P}$ = 1682 Hz) and 66.5 ($^1J_{Pt-P}$ = 1372 Hz)). Minor signals attributable to dimer **12b** were observed by ^1H and ^{31}P NMR spectroscopy in toluene-d_8. X-ray structure analysis as well as solid-state CP/MAS NMR spectroscopy revealed that the crystals formed from a toluene solution are not monomer **11b** but dimer **12b**.

Complexes **11a/12a** and **11b/12b** are in equilibrium in solution. The equilibrium is solvent dependent, and equilibrium constants, K_{eq} (= [**12**]/[**11**]^2), at 300 K for **11a/12a** are 2.4 M^{-1} and >100 M^{-1} in dichloromethane-d_2 and toluene-d_8,[16] respectively, and that for **11b/12b** is 1.2 M^{-1} in toluene-d_8. In dichloromethane-d_2 and THF-d_8 (∼0.1 M solution), signals corresponding to dimer **12b** are not detectable in NMR spectroscopy, showing the equilibrium between **11b** and **12b** shifts almost completely to the monomer **11b**. Thermodynamic parameters of the equilibrium were determined by variable-temperature NMR measurement in dichloromethane-d_2 for **11a/12a** and in toluene-d_8 for **11b/12b** and are summarized in Table 1.

Table 1. Thermodynamic Parameters for the Equilibrium between Mononuclear Complexes 11a,b and Dinuclear Complexes 12a,b[a]

complexes	$\Delta H°$, kJ mol^{-1}	$\Delta S°$, K^{-1} mol^{-1}	$\Delta G°_{300}$, kJ mol^{-1}
11a/12a[b]	−42 ± 1	−134 ± 2	−2.2 ± 0.1
11b/12b[c]	−46 ± 2	−153 ± 6	−0.4 ± 0.1

[a] Determined from the temperature dependence of K_{eq} using a van't Hoff plot. [b] In dichloromethane-d_2. [c] In toluene-d_8.

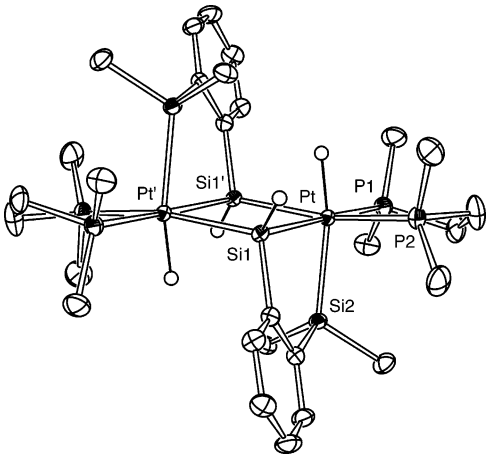

Figure 4. Molecular structure of **12a** (50% probability level). Hydrogen atoms bound to carbon atoms are omitted for clarity.

Figure 4 shows the molecular structure of complex **12a**. Selected bond lengths and angles for **12a** and **12b** are summarized in Table 2. $(Pt-Si)_2$ four-membered cycles can be classified in two categories: one has a short Si···Si diagonal distance and the other has a short Pt···Pt diagonal distance.[2−7,10a] So far all known $(Pt-Si)_2$ four-membered cycles that have two monodentate phosphine ligands (or one chelating phosphine ligand)

(15) Simulation was performed using the gNMR software package (Adept Scientific plc), and the following coupling constants were taken from the observed spectrum: $^1J(Pt-P(A)) = {}^1J(Pt'-P(A')) = 970$ Hz; $^3J(Pt'-P(A)) = {}^3J(Pt-P(A')) = 201$ Hz; $^1J(Pt-P(B)) = {}^1J(Pt'-P(B')) = 1100$ Hz; $^3J(Pt'-P(B)) = {}^3J(Pt-P(B')) = 239$ Hz; $^4J(P(A)-P(A')) = 36$ Hz; $^4J(P(B)-P(B')) = 50$ Hz. $^2J(P(A)-P(B))$, $^2J(P(A')-P(B'))$, $^4J(P(A)-P(B'))$, and $^4J(P(A')-P(B))$ were judged to be relatively small and were set to 0 in this simulation.

(16) Due to the low solubility of **12a** in toluene-d_8, accurate determination of K_{eq} for the equilibrium between **11a** and **12a** in this solvent has not been accomplished.

Table 2. Selected Bond Lengths (Å) and Angles (deg) in 12a and 12b

	12a	12b
Si1···Si1′	2.832(1)	2.792(2)
Pt···Pt′	3.8444(2)	3.8863(2)
Pt−Si1	2.3888(9)	2.394(1)
Pt−Si1′	2.3862(9)	2.391(1)
Pt−Si2	2.4124(9)	2.433(1)
Pt−P1	2.3300(9)	2.359(1)
Pt−P2	2.327(1)	2.370(1)
Si1−Pt−Si1′	72.76(3)	71.40(5)
Pt−Si1−Pt′	107.24(4)	108.60(6)
Si1−Pt−Si2	82.72(3)	82.09(5)
P1−Pt−P2	85.74(3)	85.16(5)
P1−Pt−Si1′	104.21(3)	105.04(5)
P2−Pt−Si1	97.76(3)	98.25(5)

on each of the Pt centers fall in the former category. Complexes **12a** and **12b**, having a chelating phosphine ligand on each of the Pt centers, also belong to the former one. The Si···Si distances in $(Pt^{II}-Si)_2$ four-membered cycles **14** so far reported range from 2.55 to 2.73 Å,[3,4,6,7] which are almost the same as or shorter than the longest Si−Si single bond found in $^tBu_3Si-Si^tBu_3$ (2.70 Å).[17] The Si···Si distance in the mixed-valent $Pt^{II}Pt^{IV}Si_2$ four-membered cycle **7** (2.72 Å)[10a] is at the longest end of that found in $(Pt^{II}-Si)_2$, while that in $(Pt^{IV}-Si)_2$ four-membered cycle **15** is much longer, 2.88 Å.[4] Each of **12a** and **12b** has two $(Si)_3(H)Pt^{IV}$ centers as in **15**, and the Si···Si distances in them (2.83 and 2.79 Å, respectively) are between those in **7** and **15**. These short Si···Si separations found in $(Pt-Si)_2$ four-membered cycles imply a possibility of bonding interaction between these Si atoms, and several theoretical calculations have been reported.[18−20] Recent reports on a model complex by Sakaki's group suggested that the bonding interaction between the Si atoms in these Pt complexes is weak.[20]

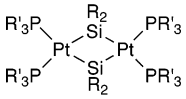

14

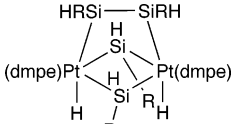

15

The molecular structure of μ-dmpe-bridged dinuclear complex **13** is shown in Figure 5. Selected bond lengths and angles for **13** are summarized in Table 3. Similar μ-dmpe-bridged dimers of bis(silyl)platinum(II) complexes were described in the literature,[4] although details of the structure were not reported. We reported similar palladium and nickel complexes.[10b,c] Complex **13** has two pentacoordinate platinum centers, which have square pyramidal geometry with a phosphorus atom at the apical position. The apical Pt−P bond (2.39 Å) is considerably longer than the equatorial Pt−P bonds (2.31 Å). Pentacoordinate platinum(II) complexes are relatively rare.[21]

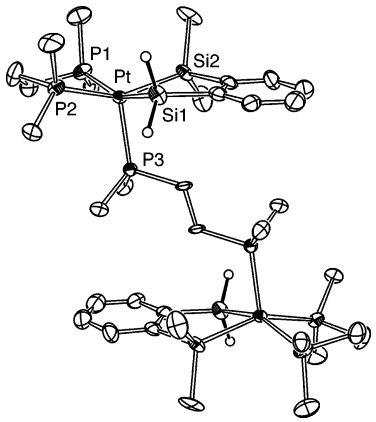

Figure 5. Molecular structure of **13** (50% probability level). Hydrogen atoms bound to carbon atoms are omitted for clarity.

Table 3. Selected Bond Lengths (Å) and Angles (deg) in 13[a]

Pt−Si1	2.343(4), 2.357(5)
Pt−Si2	2.384(5), 2.389(5)
Pt−P1	2.303(4), 2.315(5)
Pt−P2	2.306(4), 2.313(5)
Pt−P3	2.384(4), 2.403(5)
Si1−Pt−Si2	80.9(2), 80.9(2)
P1−Pt−P2	83.8(2), 84.1(2)
P1−Pt−P3	107.7(2), 103.3(2)
P2−Pt−P3	109.3(2), 108.5(2)
Si1−Pt−P1	156.4(2), 160.5(2)
Si1−Pt−P2	89.1(2), 89.3(2)
Si1−Pt−P3	95.9(2), 96.2(2)
Si2−Pt−P1	94.8(2), 94.2(2)
Si2−Pt−P2	151.5(2), 145.4(2)
Si2−Pt−P3	98.2(2), 105.5(2)

[a] Two independent molecules are present in a unit cell.

The reaction of **8** and **9a** in 2:1 ratio in toluene at room temperature afforded tris(silyl)(hydrido)bis(phosphine)platinum(IV) complexes as a mixture of two isomers **16** and **17** in 5:3 ratio. This result is similar to the reaction of **3** with $Pt(PEt_3)_3$, but different from the reaction of **8** with $Ni(dmpe)_2$, which was accompanied by Si−Si bond formation, giving complex **20**.[10d] The $^{31}P\{^1H\}$ NMR spectrum in C_6D_6 showed a pair of doublets with relatively small $^1J_{Pt-P}$ values typical for silylplatinum(IV) species;[10a,22] $^1J_{Pt-P}$ = 999 and 1428 Hz for the major isomer and $^1J_{Pt-P}$ = 1023 and 1159 Hz for the minor isomer. Pt−*H* signals in the ^1H NMR spectrum are a broad doublet ($^2J_{P-H}$ = 182 Hz) for the major isomer and a triplet ($^2J_{P-H}$ = 18 Hz) for the minor isomer. This suggests that one P atom is *trans* and the other P atom is *cis* to the hydrido ligand in the major isomer and both P atoms are *cis* to the hydrido ligand in the minor isomers. ^{29}Si and $^{29}Si\{^1H\}$ NMR spectra clearly showed the presence of an unreacted $SiMe_2H$ group in both isomers; a signal for the silicon atom with one directly connected hydrogen (a broad doublet in the ^{29}Si NMR spectrum, $^1J_{H-Si}$ = ca. 190 Hz) was respectively observed at −19.21 ppm (J_{Pt-Si} = 6 Hz) for the major isomer and at −19.02 ppm (J_{Pt-Si} = 7 Hz) for the

(17) Wieberg, N.; Schuster, H.; Simon, A.; Peters, K. *Angew. Chem., Int. Ed. Engl.* **1986**, *25*, 79.

(18) Anderson, A. B.; Shiller, P.; Zarate, E. A.; Tessier-Youngs, C. A.; Youngs, W. J. *Organometallics* **1989**, *8*, 2320−2322.

(19) Aullon, G.; Alemany, P.; Alvarez, S. *J. Organomet. Chem.* **1994**, *478*, 75−82.

(20) (a) Sakaki, S.; Yamaguchi, S.; Musashi, Y.; Sugimoto, M. *J. Organomet. Chem.* **2001**, *635*, 173−186. (b) Nakajima, S.; Yokogawa, D.; Nakao, Y.; Sato, H.; Sakaki, S. *Organometallics* **2004**, *23*, 4672−4681.

(21) For example, see: (a) Chui, K. M.; Powell, H. M. *J. Chem. Soc., Dalton Trans.* **1974**, 1879−1889. (b) Cecconi, F.; Ghilardi, C. A.; Midollini, S.; Moneti, S.; Orlandini, A.; Scapacci, G. *Inorg. Chim. Acta* **1991**, *189*, 105−110. (c) Otto, S.; Roodt, A. *Inorg. Chem. Commun.* **2001**, *4*, 49−52.

(22) Grundy, S. L.; Holmessmith, R. D.; Stobart, S. R.; Williams, M. A. *Inorg. Chem.* **1991**, *30*, 3333−3337.

Scheme 4

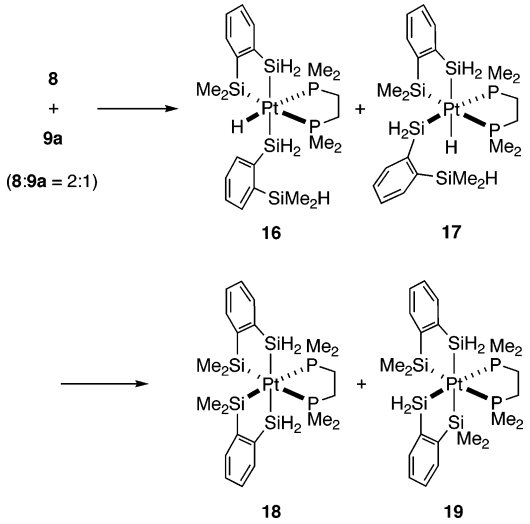

minor isomer in the $^{29}Si\{^1H\}$ NMR spectrum. The small J_{Pt-Si} values suggest no direct interaction between these Si atoms and Pt atoms. The $Me_2\mathit{Si}Pt$ signal in each isomer appeared as a doublet of doublets with a large (ca. 140 Hz) and a small (7−9 Hz) $^2J_{P-Si}$ value, indicating the Me_2Si groups have one *cis* and one *trans* P atom in both isomers. From these NMR data, the structures of the major isomer **16** and the minor isomer **17** can be assigned as shown in Scheme 4. Signals for $\mathit{Si}H_2$ groups in the $^{29}Si\{^1H\}$ NMR spectrum are also consistent with these assignment; the major isomer showed two $\mathit{Si}H_2$ signals (a triplet and a doublet of doublets) with small $^2J_{P-Si}$ values (12−18 Hz), suggesting that both of the SiH_2 groups are in *cis*-position relative to both of the P atoms. On the other hand, the minor isomer showed two doublets of doublets signals for $\mathit{Si}H_2$ groups, one of which had a large (155 Hz) and a small (15 Hz) $^2J_{P-Si}$ value and the other had small $^2J_{P-Si}$ values (10 and 12 Hz), suggesting that one of the SiH_2 groups is in *cis*-position relative to one P atom and in *trans*-position relative to the other P atom, while the other SiH_2 group is in *cis*-position relative to both of the P atoms. Crystallization of the mixture from toluene afforded X-ray quality single crystals only for the minor isomer, and its structure was unambiguously confirmed (vide infra). Judging from the $^{31}P\{^1H\}$ NMR spectrum of the reaction mixture, which showed some unidentified signals with very weak intensity, the amount of other isomers (six possible isomers, **21** and **22**) is very low (<2%) even if they are present. Selective formation of the two isomers **16** and **17** can be mainly attributed to

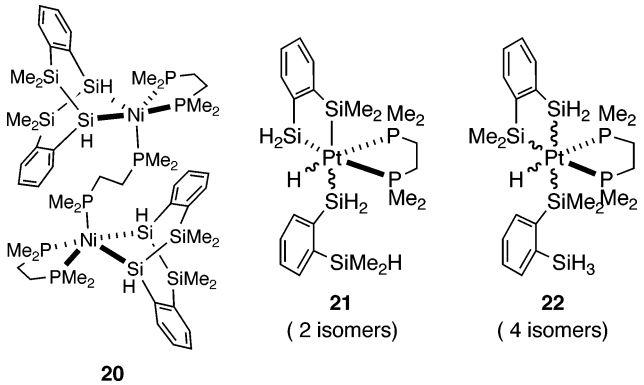

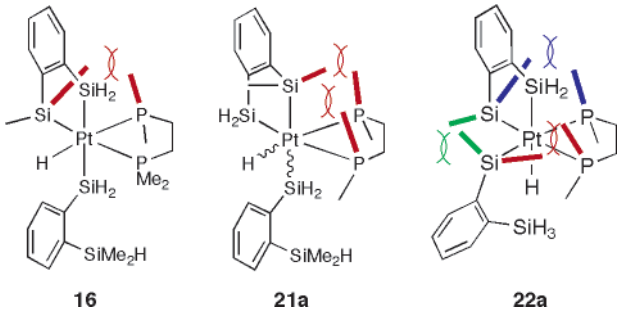

Figure 6. Schematic drawings showing steric repulsions between methyl groups in complexes **16**, **21a**, and **22a**.

the steric repulsion caused by methyl groups on silicon and phosphorus atoms. Analysis of molecular structures of complexes **16**, **18**, and **19** determined by X-ray diffraction (vide infra) suggests that severe steric repulsion is present between some of the methyl groups on silicon and phosphorus atoms in complexes **16**−**22**. Such steric repulsion is found between one pair of methyl groups in complexes **16** and **17** (e.g., see **16** in Figure 6), while between two pairs of methyl groups in complexes **21** (e.g., see **21a** in Figure 6) and between three or four pairs of methyl groups in complexes **22** (e.g., see **22a** in Figure 6).

As expected, further dehydrogenative cyclization of **16** and **17** to **18** and **19**, respectively, was much more difficult than that of **5a** and **5b** to **6**, but slowly took place at 100 °C. Monitoring of the reaction progress by NMR spectroscopy showed that even after 6 days at 100 °C, small amounts of **16** and **17** still remained and that some unidentified byproducts were formed in addition to **18** and **19**. The $^{31}P\{^1H\}$ NMR spectrum of the mixture of **18** and **19** showed two singlet signals; one is for **18**, having one set of platinum satellites ($^1J_{Pt-P} = 1037$ Hz), and the other is for **19**, having two sets of platinum satellites with P−P coupling ($^2J_{P-P} = 16$ Hz) because the two P atoms in **19** are not equivalent and $^1J_{Pt-P}$ values are different (945 and 1283 Hz, respectively). Fortunately, crystallization of the product mixture from toluene afforded X-ray quality single crystals for both isomers as a mixture, and their structures were unambiguously confirmed (vide infra).

Figures 7−9 show the molecular structures of complexes **17**, **18**, and **19**, respectively. Selected bond lengths and angles for them are summarized in Table 4. Structure determination of a complex similar to **17**, *fac*-(dmpe)Pt(H)(SiH_2Ph)$_3$, was reported by Tilley,[4] while the structures of **5a** and **5b** have not been determined by X-ray analysis. Molecular structures of two tetrakis(silyl)platinum(IV) complexes, **6**[10a] and **23**,[23] have been reported. The Pt atom in **17** has a distorted octahedral geometry. The Pt−Si bond lengths in **17** are within a normal range.[1c] The longest Pt−Si bond in **18** and **19** is the $SiMe_2$−Pt bond *trans* to a silyl group (Pt−Si_4 in **19**, 2.451(1) Å), which is shorter than the Si−Pt bonds in **23** (average 2.475(9) Å) that accommodate four bulky silyl groups with two isocyanide ligands in *trans* arrangement. Since in **18** and **19**, $SiMe_2$−Pt and SiH_2−Pt bonds under very similar environment are present, they are a good example for the comparison of $SiMe_2$−

(23) Suginome, M.; Oike, H.; Shuff, P. H.; Ito, Y. *J. Organomet. Chem.* **1996**, *521*, 405−408.

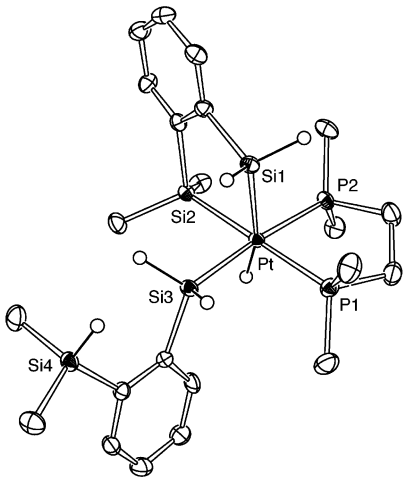

Figure 7. Molecular structure of **17** (50% probability level). Hydrogen atoms bound to carbon atoms are omitted for clarity.

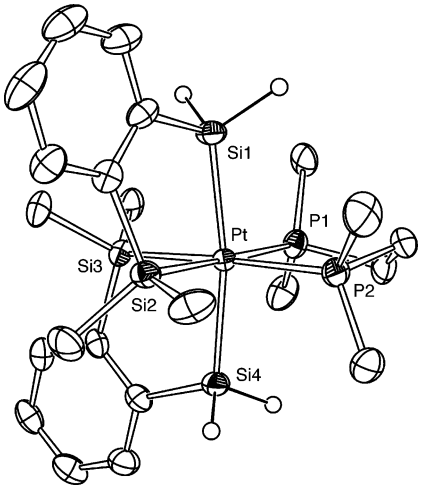

Figure 8. Molecular structure of **18** (50% probability level). Hydrogen atoms bound to carbon atoms are omitted for clarity.

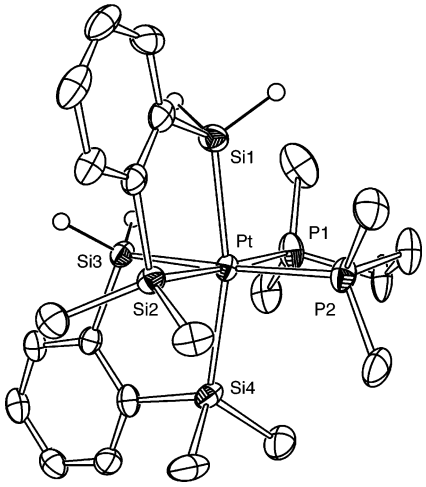

Figure 9. Molecular structure of **19** (50% probability level). Hydrogen atoms bound to carbon atoms are omitted for clarity.

Pt and SiH_2–Pt bond lengths. With regard to the Pt–Si bonds *trans* to a silyl group, the Pt–$SiMe_2$ bond (2.451(1) Å) is 0.04–0.05 Å longer than the Pt–SiH_2 bonds (2.398(2)–2.413(1) Å). A similar difference is also found in Pt–Si bonds *trans* to a phosphine; the Pt–$SiMe_2$ bond (2.403(2)–2.406(1) Å) is ca. 0.04 Å longer than Pt–SiH_2 bonds (2.368(1) Å). Judging from the molecular structures of **18** and **19** determined by X-ray analysis, the main factor causing the difference in Pt–$SiMe_2$ and Pt–SiH_2 bond lengths is probably the steric repulsion between the methyl groups on silicon and phosphorus atoms.

Table 4. Selected Bond Lengths (Å) and Angles (deg) in 17, 18, and 19[a]

	17	18[a]	19
Pt–Si1	2.388(1)	2.406(2), 2.394(2)	2.413(1)
Pt–Si2	2.393(1)	2.404(2), 2.401(2)	2.404(1)
Pt–Si3	2.371(1)	2.406(1), 2.406(1)	2.368(1)
Pt–Si4		2.394(2), 2.402(2)	2.451(1)
Pt–P1	2.346(1)	2.356(1), 2.362(2)	2.344(1)
Pt–P2	2.334(1)	2.358(2), 2.358(1)	2.347(1)
Si1–Pt–Si2	84.59(5)	83.79(5), 84.66(6)	83.59(4)
Si1–Pt–Si3	86.62(5)	88.18(5), 86.83(5)	84.10(4)
Si1–Pt–Si4		170.35(5), 169.13(5)	166.32(4)
Si2–Pt–Si3	90.80(5)	87.50(5), 86.45(5)	89.15(4)
Si2–Pt–Si4		89.63(5), 88.56(5)	88.88(4)
Si3–Pt–Si4		84.48(5), 84.27(5)	84.38(4)
P1–Pt–P2	84.81(5)	84.53(5), 84.85(5)	85.20(4)
Si1–Pt–P1	95.58(5)	94.79(5), 95.18(6)	93.70(4)
Si1–Pt–P2	95.23(5)	94.70(5), 93.12(5)	93.66(4)
Si2–Pt–P1	179.31(5)	178.16(4), 178.92(4)	177.20(4)
Si2–Pt–P2	94.52(5)	94.41(5), 94.09(5)	95.69(4)
Si3–Pt–P1	89.88(5)	93.63(5), 94.61(5)	89.84(4)
Si3–Pt–P2	174.51(5)	176.70(5), 179.45(6)	174.42(4)
Si4–Pt–P1		91.93(5), 91.76(6)	93.62(4)
Si4–Pt–P2		92.84(6), 95.83(5)	98.45(4)

[a] Two independent molecules are present in a unit cell.

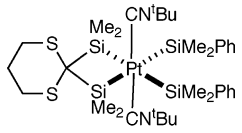

23

Conclusions

The reaction of 1,2-$C_6H_4(SiMe_2H)(SiH_3)$ (**8**), a hybrid of 1,2-$C_6H_4(SiMe_2H)_2$ **1** and 1,2-$C_6H_4(SiH_3)_2$ **3**, with platinum(0) phosphine complexes has been investigated. It is more complicated than that of **1**, but similar to that of **3**. The main difference in the reactions of **8** and **3** is the behavior of bis(silyl)platinum(II) complexes derived from them. Bis(silyl)platinum(II) complexes **11a** and **11b** have been disclosed to be in equilibrium with their dimers **12a** and **12b**, respectively. This type of equilibrium has never been reported in related silylplatinum complexes. The reaction of hydrosilane **8** with Pt complex **9a** or **10a** in 2:1 ratio proceeded similarly to that of **3** with $Pt(PEt_3)_3$, giving tris(silyl)(hydrido)-platinum(IV) complexes **16** and **17**. Further intramolecular dehydrogenative cyclization of **16** and **17** to form tetrakis(silyl)platinum(IV) complexes **18** and **19** took place but required higher reaction temperature and longer reaction time than that of less bulky tris(silyl)-(hydrido)platinum(IV) complexes **5a** and **5b** derived from **3**.

Experimental Section

General Procedures. All manipulations of air-sensitive materials were carried out under a nitrogen atmosphere using standard Schlenk tube techniques or in a glovebox filled with

argon. Toluene, toluene-d_8, THF-d_8, and benzene-d_6 were distilled from Na/benzophenone ketyl. Dichloromethane-d_2 was distilled from CaH_2. All other anhydrous solvents were purchased from Kanto Chemicals or Aldrich. Compound **8** was prepared as described previously.[10d] ^{1}H, ^{29}Si, and ^{31}P NMR spectra were recorded on JEOL LA500 (for solution NMR) and Bruker ARX300 (for solid-state NMR) spectrometers. Chemical shifts are given in ppm using external references (for solution NMR spectra, tetramethylsilane (0 ppm) for ^{1}H and ^{29}Si and 85% H_3PO_4 (0 ppm) for ^{31}P; for solid-state NMR spectra, 85% H_3PO_4 (0 ppm) for ^{31}P and DSS (sodium 4,4-dimethyl-4-silapentanesulfonate, 1.534 ppm) for ^{29}Si), and coupling constants are reported in hertz.

[{1,2-C$_6$H$_4$(SiMe$_2$)(SiH$_2$)}Pt(dmpe)] (11a) and [(dmpe)-Pt^{IV}(H){1,2-C$_6$H$_4$(SiMe$_2$)(μ-SiH)]$_2$ (12a). A mixture of Pt(PEt$_3$)$_4$ (500 mg, 0.75 mmol) and dmpe (113 mg, 0.75 mmol) in toluene (3 mL) was stirred at room temperature for 40 min to give Pt(PEt$_3$)$_2$(dmpe), **9a**. After removal of volatiles under vacuum, the residual **9a** was dissolved in toluene (4 mL). Hydrosilane **8** (117 mg, 0.70 mmol) was added to the toluene solution of **9a** at 0 °C, and the mixture was stirred at room temperature for 24 h. After removal of volatiles under vacuum, the residue was washed with hexane (3 × 2 mL) and dried under vacuum to give a colorless solid. Yield: 92% (330 mg). NMR analysis of this solid in THF-d_8 showed high purity of the products (molar ratio of **11a/12a** was ca. 95/5 in THF-d_8). Single crystals of **12a** suitable for X-ray analysis were obtained by the recrystallization of the solid from toluene, THF, or DMF. For **11a**: ^{1}H NMR (THF-d_8, 499.1 MHz): δ 0.38 (6H, d, $^4J_{P-H}$ = 3, $^3J_{Pt-H}$ = 23, Si*Me*), 1.51−1.62 (12H, m, P*Me*), 1.67−1.82 (4H, m, PCH_2CH_2P), 5.53 (2H, t, $^3J_{P-H}$ = 7, $^1J_{Si-H}$ = 159, $^2J_{Pt-H}$ = 22), 7.01−7.07 (2H, m), 7.45 (1H, d, J = 7), 7.58 (1H, d, J = 7). ^{31}P{^{1}H} NMR (THF-d_8, 202.0 MHz): δ 39.5 (d, $^2J_{P-P}$ = 13, $^1J_{Pt-P}$ = 1623), 40.0 (d, $^2J_{P-P}$ = 13, $^1J_{Pt-P}$ = 1337). For **12a**: CP-MAS ^{31}P{^{1}H} NMR (121.5 MHz): −5.0 ($^1J_{Pt-P}$ = 1074), 1.0 ($^1J_{Pt-P}$ = 994). CP-MAS ^{29}Si{^{1}H} NMR (59.6 MHz): −94.0 (quasi septet, J = 125), 0.7 ($^1J_{Pt-Si}$ = 757). ^{1}H NMR (THF-d_8, 499.1 MHz): δ −8.61 (Pt−*H*). ^{31}P NMR (THF-d_8, 202.0 MHz): δ −10.3 ($^1J_{Pt-P}$ = 1102, $^3J_{Pt-P}$ = 239), −5.9 ($^1J_{Pt-P}$ = 971, $^3J_{Pt-P}$ = 201). Anal. Calcd for $C_{28}H_{56}P_4Pt_2Si_4$: C, 33.00; H, 5.54. Found: C, 33.56; H, 5.46.

[{1,2-C$_6$H$_4$(SiMe$_2$)(SiH$_2$)}Pt(depe)] (11b) and [(depe)-Pt^{IV}(H){1,2-C$_6$H$_4$(SiMe$_2$)(μ-SiH)]$_2$ (12b). A mixture of Pt(PEt$_3$)$_4$ (167 mg, 0.25 mmol) and depe (103 mg, 0.50 mmol) in hexane (3 mL) was stirred at room temperature for 1 h to give Pt(depe)$_2$ **10b**. After removal of volatiles under vacuum, the residual **10b** was dissolved in benzene (3 mL). Hydrosilane **8** (41 mg, 0.25 mmol) was added to the benzene solution of **10b** at room temperature and stirred at room temperature for 24 h. After removal of volatiles under vacuum, the residue was dissolved in toluene-d_8 for NMR measurement, showing the formation of **11b** and **12b** (the ratio of **11b/12b** by ^{31}P NMR integration was ca. 7:1). Keeping the NMR sample at room temperature for 24 h afforded colorless crystals of **12b**, which was separated by filtration, washed with hexane, and dried under vacuum. Yield: 59% (84 mg). For **11b**: ^{1}H NMR (THF-d_8, 499.1 MHz): δ 0.40 (6H, d, $^4J_{P-H}$ = 3, $^3J_{Pt-H}$ = 23, Si*Me*), 1.05−1.13 (12H, m, PCH$_2$CH_3), 1.74−2.24 (12H, m, PCH_2CH_2P and PCH_2CH$_3$), 5.56 (2H, t, $^3J_{P-H}$ = 7, $^1J_{Si-H}$ = 159, $^2J_{Pt-H}$ = 24), 7.01−7.08 (2H, m), 7.46 (1H, d, J = 7), 7.58 (1H, d, J = 7). ^{31}P{^{1}H} NMR (THF-d_8, 202.0 MHz): δ 64.5 (d, $^2J_{P-P}$ = 13, $^1J_{Pt-P}$ = 1682), 66.5 (d, $^2J_{P-P}$ = 13, $^1J_{Pt-P}$ = 1372). For **12b**: CP-MAS ^{31}P{^{1}H} NMR (121.5 MHz): 1.2 ($^1J_{Pt-P}$ = 949), 10.4 ($^1J_{Pt-P}$ = 1044). CP-MAS ^{29}Si{^{1}H} NMR (59.6 MHz): −94.5, −3.1 ($^1J_{Pt-Si}$ = 767). ^{31}P NMR (toluene-d_8, 202.0 MHz): δ 13.0 ($^1J_{Pt-P}$ = 923, $^3J_{Pt-P}$ = 194), 18.0 ($^1J_{Pt-P}$ = 1065, $^3J_{Pt-P}$ = 224). Anal. Calcd for $C_{36}H_{72}P_4Pt_2Si_4$: C, 38.22; H, 6.41. Found: C, 38.50; H, 6.37.

[{1,2-C$_6$H$_4$(SiMe$_2$)(SiH$_2$)}Pt(dmpe)]$_2$(μ-dmpe) (13). A mixture of **11a/12a** (20 mg, 0.039 mmol as **11a**) and excess dmpe (58 mg, 0.39 mmol) in toluene (2 mL) was stirred at room temperature for 12 h. After filtration, the solution was cooled to −30 °C to give a small amount of single crystals suitable for X-ray analysis. This compound was characterized only by X-ray analysis.

[{1,2-C$_6$H$_4$(SiMe$_2$H)(SiH$_2$)}{1,2-C$_6$H$_4$(SiMe$_2$)(SiH$_2$)}(H)-Pt^{IV}(dmpe)] (16 and 17). Pt(PEt$_3$)$_2$(dmpe) was prepared from Pt(PEt$_3$)$_4$ (250 mg, 0.37 mmol) and dmpe (56 mg, 0.37 mmol) as described above and dissolved in toluene (4 mL). To this solution was added hydrosilane **8** (125 mg, 0.75 mmol) at 0 °C, and the mixture was stirred at room temperature for 24 h. Removal of volatiles under vacuum afforded a light yellow residue, which was washed with hexane (3 × 2 mL) and dried under vacuum to give a mixture of **16** and **17** (5:3 judged by ^{1}H NMR integration) as a colorless solid, 179 mg (78%). ^{1}H NMR (benzene-d_6, 499.1 MHz): δ −10.03 (br d, $^2J_{P-H}$ = 182, $^1J_{Pt-H}$ = 847, Pt−*H* for **16**), −8.30 (t, $^2J_{P-H}$ = 18, $^1J_{Pt-H}$ = 808, Pt−*H* for **17**), 0.42 (dd, J = 4, 16, CH_3 × 2 for **17**), 0.58 (dd, J = 4, 17, CH_3 × 2 for **16**), 0.76−1.25 (m, CH_3 × 6 and PCH_2CH_2P for **16** and **17**), 4.30−5.35 (m, SiH_2 × 2 for **16** and **17**), 7.18−7.25 (m, aromatic-*H* × 3 for **16** and **17**), 7.32 (quasi t, J = 8, aromatic-*H* × 1 for **16**), 7.43 (quasi t, J = 7, aromatic-*H* × 1 for **17**), 7.62−7.71 (m, aromatic-*H* × 2 for **16** and **17**), 8.06 (d, J = 7, aromatic-*H* × 1 for **17**), 8.12−8.14 (m, aromatic-*H* × 1 for **16**), 8.34 (d, J = 8, aromatic-*H* × 1 for **16**), 8.75 (d, J = 7, aromatic-*H* × 1 for **17**). ^{31}P{^{1}H} NMR (benzene-d_6, 202.0 MHz): for **16**, δ −19.77 (d, $^2J_{P-P}$ = 8, $^1J_{Pt-P}$ = 999), −15.61 (d, $^2J_{P-P}$ = 8, $^1J_{Pt-P}$ = 1428); for **17**, δ −12.83 (d, $^2J_{P-P}$ = 17, $^1J_{Pt-P}$ = 1023), −11.43 (d, $^2J_{P-P}$ = 17, $^1J_{Pt-P}$ = 1159). ^{29}Si{^{1}H} NMR (benzene-d_6, 99.1 MHz): for **16**, δ −48.8 (dd, $^2J_{P-Si}$ = 12, 18, $^1J_{Pt-Si}$ = 685, *Si*H$_2$), −34.8 (t, $^2J_{P-Si}$ = 13, $^1J_{Pt-Si}$ = 592, *Si*H$_2$), −19.2 (s, $^4J_{Pt-Si}$ = 6, *Si*Me$_2$H), 8.2 (dd, $^2J_{P-Si}$ = 7, 138, $^1J_{Pt-Si}$ = 641, *Si*Me$_2$Pt); for **17**, δ −37.5 (dd, $^2J_{P-Si}$ = 15, 155, $^1J_{Pt-Si}$ = 746, *Si*H$_2$), −25.4 (dd, $^2J_{P-Si}$ = 10, 12, $^1J_{Pt-Si}$ = 643, *Si*H$_2$), −19.0 (s, $^4J_{Pt-Si}$ = 7, *Si*Me$_2$H), 6.5 (dd, $^2J_{P-Si}$ = 10, 141, $^1J_{Pt-Si}$ = 671, *Si*Me$_2$Pt). Anal. (for the mixture of **16** and **17**) Calcd for $C_{22}H_{42}P_2PtSi_4$: C, 39.09; H, 6.26. Found: C, 39.28; H, 6.24.

[{1,2-C$_6$H$_4$(SiMe$_2$)(SiH$_2$)}$_2$Pt^{IV}(dmpe)] (18 and 19). A solution of complexes **16** and **17** (100 mg, 0.15 mmol) in toluene (3 mL) was heated at 100 °C for 6 days. Removal of volatiles under vacuum left a light yellow solid. Washing the solid with hexane (3 × 2 mL) followed by drying under vacuum afforded a mixture of **18** and **19** as a colorless solid. Yield: 77% (77 mg). Further purification was performed by the recrystallization from toluene to give X-ray quality single crystals. ^{1}H NMR (toluene-d_8, 499.1 MHz): δ 0.44 (d, $^4J_{P-H}$ = 2, $^3J_{Pt-H}$ = 18, SiCH_3 × 2 for **18**), 0.52 (s, $^3J_{Pt-H}$ = 8, SiCH_3 × 1 for **19**), 0.57 (d, $^4J_{P-H}$ = 2, $^3J_{Pt-H}$ = 20, SiCH_3 × 1 for **19**), 0.70 (t, $^4J_{P-H}$ = 3, $^3J_{Pt-H}$ = 15, SiCH_3 × 2 for **18**), 0.75 (dd, $^4J_{P-H}$ = 2, 3, $^3J_{Pt-H}$ = 15, SiCH_3 × 1 for **19**), 0.70 (s, $^3J_{Pt-H}$ = 12, SiCH_3 × 1 for **19**), 0.84−1.21 (m, PCH_3 × 4 and PCH_2CH_2P for **18** and **19**), 4.05−4.65 (m, SiH_2 × 2 for **18** and **19**), 7.13−8.07 (m, aromatic-*H* × 8 for **18** and **19**). ^{31}P{^{1}H} NMR (toluene-d_8, 202.0 MHz): for **18**, δ −20.69 (s, $^1J_{Pt-P}$ = 1037); for **19**, δ −20.69 (s (AA′X pattern), $^1J_{Pt-P}$ = 945, 1283, $^2J_{P-P}$ = 16). ^{29}Si{^{1}H} NMR (toluene-d_8, 99.1 MHz): for **18**, δ −26.6 (t, $^2J_{P-Si}$ = 15, $^1J_{Pt-Si}$ = 657, *Si*H$_2$), 6.9 (dd, $^2J_{P-Si}$ = 12, 133, $^1J_{Pt-Si}$ = 668, *Si*Me$_2$-Pt). Anal. (for the mixture of **18** and **19**) Calcd for $C_{22}H_{40}P_2$-$PtSi_4$: C, 39.21; H, 5.98. Found: C, 39.73; H, 5.75.

X-ray Crystallography. Data collection was performed on a Bruker Smart Apex CCD diffractometer (Mo Kα radiation, graphite monochromator) except for complex **12b**, for which the Rigaku AFC7R system (Mo Kα radiation, graphite monochromator) was used. Data were corrected for absorption. The structures were solved by the Patterson method. Structure refinement was carried out by full-matrix least squares on F^2. Table 5 gives further details. Structure solution and refinement were performed using the CrystalStructure software

Table 5. Crystallographic Data for 12a, 12b, 13, 17, 18, and 19

	12a	12b	13	17	18	19
formula	$C_{28}H_{56}P_4Pt_2Si_4$	$C_{36}H_{72}P_4Pt_2Si_4$	$C_{34}H_{72}P_6Pt_2Si_4$	$C_{22}H_{42}P_2Pt_1Si_4$	$C_{22}H_{40}P_2Pt_1Si_4$	$C_{22}H_{40}P_2Pt_1Si_4$
fw	1019.17	1131.38	1169.31	675.95	673.94	673.94
cryst size	0.08 × 0.08 × 0.05	0.20 × 0.13 × 0.07	0.11 × 0.09 × 0.06	0.18 × 0.10 × 0.03	0.17 × 0.16 × 0.01	0.22 × 0.19 × 0.11
cryst syst	monoclinic	monoclinic	monoclinic	monoclinic	monoclinic	orthorhombic
space group	$P2_1/n$ (No. 14)	$P2_1/n$ (No. 14)	$P\bar{1}$ (No. 2)	$P2_1/c$ (No. 14)	$P2_1/c$ (No. 14)	$P2_12_12_1$ (No. 19)
a/Å	9.3844(5)	10.675(3)	9.289(1)	9.6262(5)	16.8631(8)	8.8429(5)
b/Å	9.1907(4)	18.534(3)	14.023(2)	8.7017(5)	18.9110(9)	17.0603(9)
c/Å	21.6907(10)	11.588(2)	18.694(3)	34.260(2)	19.5125(10)	18.4900(10)
α/deg			88.214(3)			
β/deg	93.2680(10)	107.95(2)	88.025(3)	91.9570(10)	115.4060(10)	
γ/deg			76.432(2)			
V/Å	1867.8(2)	2181.1(8)	2365.1(6)	2868.1(3)	5620.7(5)	2789.4(3)
Z	2	2	2	4	8	4
D_{calc}/g cm^{-3}	1.81	1.72	1.64	1.57	1.59	1.61
F(000)	992	1120	1156	1352	2688	1344
μ(Mo Kα)/mm^{-1}	7.769	6.662	6.212	5.160	5.266	5.305
T/K	153(1)	223(2)	153(1)	153(1)	153(1)	153(1)
no. of rflns measd	10 855	5422	13 897	16 757	33 289	16 651
no. of unique rflns	4218	4993	10 079	6507	12 820	6234
no. of variables	181	218	406	287	556	279
R1 ($I_o > 2.0\sigma(I_o)$)	0.025	0.030	0.078	0.037	0.035	0.023
wR2 (all data)	0.065	0.077	0.258	0.080	0.087	0.049
GOF	1.04	1.03	1.11	1.16	1.04	0.98
diff peak, hole, e Å^{-3}	4.57, −0.96	1.39−1.38	9.77, −3.27	1.36, −1.52	1.95, −0.80	1.02, −0.38

package[24] with the SHELX-97 program.[25] Ortep drawings were generated using ORTEP-3 for Windows.[26] Crystallographic data have been deposited with the Cambridge Crystallographic Data Centre. Copies of the data can be obtained free of charge on application to CCDC, 12 Union Road, Cambridge CB2 1EZ, U.K. (fax, (internat.) +44-1223/336-033; e-mail, data_request@ccdc.cam.ac.uk), on quoting the deposition numbers CCDC-273818 (**12a**), CCDC-273819 (**12b**), CCDC-273820 (**13**), CCDC-273821 (**17**), CCDC-273822 (**18**), and CCDC-273823 (**19**).

(24) *CrystalStructure* version 3.6.0; Rigaku Corparation and Rigaku/MSC, 2004.

(25) Sheldrick, G. M. *SHELXL-97*; Universität Göttingen: Germany, 1997.

(26) Farrugia, L. J. *J. Appl. Crystallogr*. **1997**, *30*, 565.

Acknowledgment. This work was supported by a Grant-in-Aid for Scientific Research (No. 15350037) from the Ministry of Education, Science, Sports and Culture, Japan, and the Japan Science and Technology Corporation (JST) through the CREST program. M.L.N.R. thanks JST for a postdoctoral fellowship.

Supporting Information Available: X-ray crystallographic file for complexes **12a**, **12b**, **13**, **17**, **18**, and **19** in CIF format. This material is available free of charge via the Internet at http://pubs.acs.org.

OM050498J